Tetrahedron 72 (2016) 7790–7795

Contents lists available at ScienceDirect

Tetrahedron

journal homepage: www.elsevier.com/locate/tet

Intramolecular homolytic substitution in selenoxides and selenones

Amber N. Hancock [a,*], Sara H. Kyne [b], Heather M. Aitken [a], Carl H. Schiesser [a]

[a] School of Chemistry and Bio21 Molecular Science and Biotechnology Institute, The University of Melbourne, Victoria, 3010, Australia
[b] School of Chemistry, University of Lincoln, Joseph Banks Laboratories, Green Lane, Lincoln, Lincolnshire LN6 7DL, UK

ARTICLE INFO

Article history:
Received 23 May 2016
Received in revised form 24 August 2016
Accepted 30 August 2016
Available online 31 August 2016

Keywords:
Radical
Homolytic substitution
Selenium
Selenoxide
Selenone
Computational chemistry

ABSTRACT

G3(MP2)-RAD calculations provide activation energies for intramolecular homolytic substitution in the 4-(alkylselenoxo)butyl and 4-(alkylselendioxo)butyl radicals ranging from 21–39 kJ mol^{-1}, and 143–170 kJ mol^{-1} for the selenoxide and selenone, respectively. Arrhenius data translate into rate constants for ring-closure of 1.5×10^{5}–2.5×10^{8} s^{-1} (80°) for the selenoxides, and 5.4×10^{-14}–5.1×10^{-11} s^{-1} (80°) for the corresponding selenones. NBO analyses show alkyl radicals are *electrophilic* during homolytic substitution at selenoxide selenium. The dominant orbital interaction in the transition state is worth 2413 kJ mol^{-1} and involves the SOMO and the lone-pair of electrons on selenium. The corresponding selenones are calculated to ring-close through transition states in which alkyl radicals are *nucleophilic*, but involve weak (SOMO–> σ^* and SOMO–> π^*) interactions. Consequently, this chemistry is not viable for selenones because of the lack of lone-pairs of electrons on the chalcogen.

1. Introduction

Free radical methods in synthesis abound.[1] The modern practitioner has access to reliable methods for the formation of a variety of rings through intramolecular homolytic addition chemistry,[2,3] and to higher heterocycles through the application of intramolecular homolytic substitution (S_Hi) chemistry at silicon, germanium, tin, sulfur, selenium and tellurium.[4,5]

We have been involved in the design and application of homolytic substitution chemistry involving selenium and have reported the synthesis of several important selenium-containing heterocycles utilizing this chemistry.[6–9] An example of the use of this chemistry (in tandem with homolytic addition) for the preparation of a selenium-containing antihypertensive is depicted in Scheme 1.[10]

As part of this work, we have also explored the mechanism of free radical attack at the chalcogens, and determined important kinetic data for these transformations.[5,11–15] It had been generally accepted that free radical attack at higher heteroatoms occured either through a 'smooth' transition state such as **1** or **2**, or through a hypervalent intermediate such as **3**, which can undergo pseudorotation prior to dissociation.[16] In the case of silicon, germanium and tin, it has been shown that substitution can occur either by frontside (**1**) or backside (**2**) attack,[17] while reactions involving

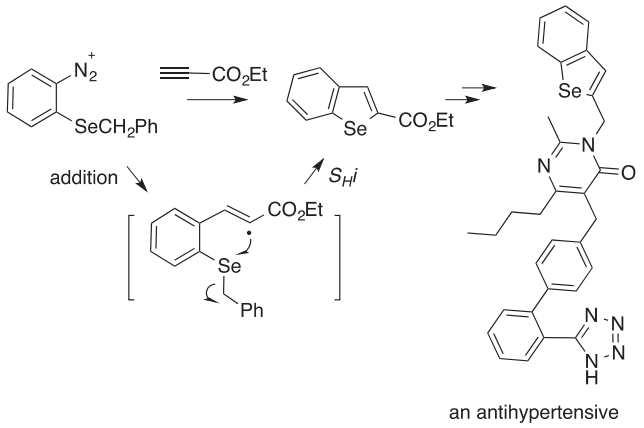

Scheme 1.

chalcogen appear to occur only via the backside pathway or (for tellurium) through an intermediate (**3**) that is too shortlived to play an important mechanistic role.[18] In each mechanism it has been assumed that the carbon-centered radical is *nucleophilic* in its substitution chemistry,[1,19] an assumption that could not adequately explain the lack of S_H2 chemistry at sulfone sulfur,[20] the system that should react most efficiently with a nucleophilic carbon-centered radical (Scheme 2). ‡ NBO analyses have been used previously by

* Corresponding author. Fax: +61 3 9347 8189; e-mail address: amber.hancock@unimelb.edu.au (A.N. Hancock).

http://dx.doi.org/10.1016/j.tet.2016.08.083
0040-4020/

us to understand the *N*-philicity of acyl radicals. It should be noted that the calculated energies contain electronic (orbital interaction) terms only and should not be confused with bond energies because they do not include the nuclear repulsion term required for determining bond strengths.

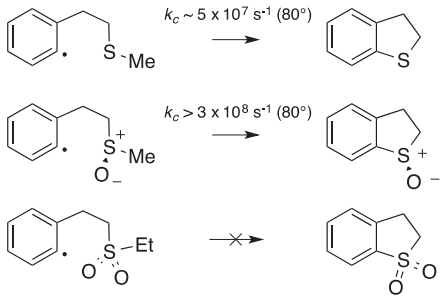

Scheme 2.

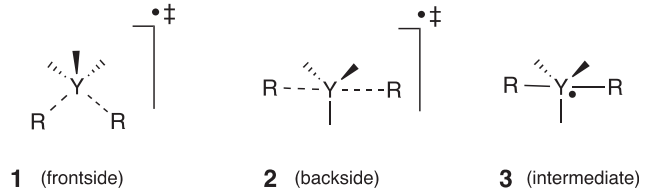

1 (frontside) **2** (backside) **3** (intermediate)

We recently reported that homolytic substitution at sulfone sulfur (devoid of lone pairs) is too slow to be competitive with other processes, in turn providing an explanation for the lack of homolytic substitution chemistry involving sulfones.[13] Indeed, NBO analyses showed that the dominant orbital interactions in the S_H2 transition states at sulfur involve at least one lone pair and this observation required a reassessment of the prevailing mechanism for S_H2 chemistry (Scheme 3).[13]

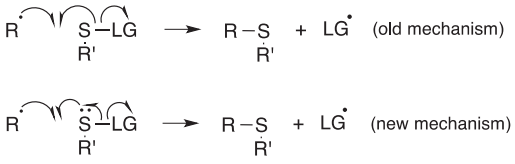

Scheme 3.

Recently, we reported the results of experimental and computational work aimed at determining important kinetic data for the ring-closures of 4-(alkylseleno)butyl and 5-(alkylseleno)pentyl radicals (examples: Scheme 4) and showed that high-level (G3(MP2)-RAD) calculations routinely provide rate constants for these homolytic substitution processes that are within error of the experimentally-determined values.

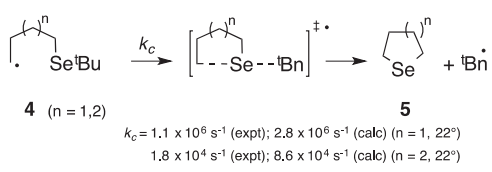

4 (n = 1,2) **5**

k_c = 1.1 x 10^6 s^{-1} (expt); 2.8 x 10^6 s^{-1} (calc) (n = 1, 22°)
1.8 x 10^4 s^{-1} (expt); 8.6 x 10^4 s^{-1} (calc) (n = 2, 22°)

Scheme 4.

Given that no experimental examples of homolytic substitution at selenoxides and selenones have been reported to date, presumably because of the intrinsic reactivity of these functional groups through alternative competing pathways,[21] we turned to computational methods to explore the effect of lone pairs and leaving groups on the cyclization of the oxides **4** to afford the tetrahydroselenophene oxides **5**. Similar to their sulfur-containing counterparts, high-level calculations reveal that S_Hi chemistry at selenides and selenoxides proceed well, while reactions at selenones have prohibitively high energy barriers. G3(MP2)-RAD calculations predict rate constants of 4.1×10^8 and 5.4×10^{-14} s^{-1} for the cyclization of the benzyl-substituted radicals **6** (R=Bn) at 80° (Scheme 5). This is to be compared to the value of 3.0×10^8 s^{-1} for the ring-closure of the 4-(benzylseleno)butyl radical at 80°.[15]

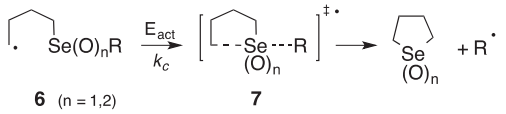

6 (n = 1,2) **7**

Scheme 5.

2. Computational methods

Ab initio and DFT calculations were carried out using Gaussian 09.[22] B3LYP/6-31G(d) optimisations were performed on starting materials **6**, transition states **7** and cyclization products as part of the G3(MP2)-RAD composite method (vide infra). BH and HLYP/6-311G(d,p) optimisations and NBO analyses were performed on transition states **9**. Geometry optimizations were performed utilizing standard gradient techniques.[23] Values of $\langle s^2 \rangle$ never exceeded 0.81 before annihilation of the first spin contaminant. After annihilation of quartet contamination $\langle s^2 \rangle$ ranged from 0.75 to 0.77. All ground and transition state structures were verified by vibrational frequency analysis. Optimized geometries and energies for all transition structures in this study are available in the Supplementary data. Kinetic parameters were determined using the Eyring equation and energies obtained using the G3(MP2)-RAD method. G3(MP2)-RAD is a high-level composite method that has been shown to perform within chemical accuracy for analogous radical reaction, hence it was selected for our study.[24]

3. Results and discussion

In order to provide insight into the intramolecular homolytic substitution process at the selenium oxides **6**, we began this study by locating the transition states **7** for the cyclization of radicals **6** at the B3LYP/6-31G(d) level of theory required for the G3(MP2)-RAD calculation.[24] Previous benchmarking studies have established that this level of theory provides reliable thermodynamic and kinetic data for free radical reactions that include homolytic substitution and addition.[14,15,25]

Vibrational frequency analysis verified structures **7** corresponds to the transition states for the homolytic substitution process. Optimized transitions states **7** are depicted in Figs. 1 and 2 with full geometric details available in the Supplementary data. Two (*syn*/*anti*)[†] stereoisomeric transition structures were located for the ring-closures of the selenoxides **7** (n=1) (Fig. 1) while only a single structure **7** (n=2) was located for each of the selenones.

Inspection of Fig. 1 reveals that the *syn* transition states **7** (n=1) have similar transition state separations to those reported previously for the cyclization of selenides **6** (n=0).[15] For example, for the benzyl-substituted system (R=Bn), B3LYP/6-31G(d) transition states separations of 2.357 and 2.157 Å are reported for the *syn* transition state **7** (n=1), with the corresponding separations in the

[†] *syn* Corresponds to a structure with the methylene group α to the bond forming carbon and the carbonyl oxygen of the same face of the molecule. *anti* Denotes a structure with them on opposite faces.